This is a peer-reviewed, accepted author manuscript of the following research article: Naraghipour, K., Ahmed, K., & Booth, C. (2021). New islanding detection method with voltage amplitude variation for inverter-based distributed generator. In *2021 9th International Conference on Smart Grid (icSmartGrid)* (pp. 243-248). [9551234]
IEEE. https://doi.org/10.1109/icSmartGrid52357.2021.9551234

New Islanding Detection Method With Voltage Amplitude Variation for Inverter-based Distributed Generator

Kianoush Naraghipour
Electronic and Electrical Department
University of Strathclyde
Glasgow, UK
kianoush.naraghipour@strath.ac.uk

Khaled Ahmed
Electronic and Electrical Department
University of Strathclyde
Glasgow, UK
khaled.ahmed@strath.ac.uk

Campbell Booth
Electronic and Electrical Department
University of Strathclyde
Glasgow, UK
campbell.d.booth@strath.ac.uk

***Abstract*— In this paper, a new islanding detection method for inverter-based distributed generator (DG) is proposed, which is based on voltage amplitude variation. The proposed method can detect islanding with zero non-detection zone (NDZ), negligible consequence on power quality and simple performance. A new formula is embedded in the active power reference equation to deviate and accelerate the point of common coupling (PCC) voltage when islanding occurs. Therefore, a passive under/over voltage relay will be sufficient to detect islanding within the voltage permissible limit. The main benefit of the presented method is its independency from the load parameters such as loading quality factor. The proposed method is modelled with computer-aided SIMULINK/MATLAB software. The presentation of the proposed method is considered for a DG system with both unity and non-unity power factors. The performance is confirmed for different loading quality factors. Furthermore, it is also validated the proposed islanding detection method under imbalance loading.**

Keywords—Distributed Generator (DG), Over/Under Voltage (OUV), Over/Under Frequency (OUF), Non-Detection Zone (NDZ), Point of Common Coupling (PCC)

I. INTRODUCTION

Unintentional islanding is an undesirable event, which occurs after the grid disconnection from a part of system, comprising distributed generator (DG) and load [1]. In accordance with IEEE 1547-2018 [2], the DG shall detect the islanding and trip in 2 s. The islanding detection methods can be classified within remote methods and local methods. Remote methods is based on a communication link from the DG to the grid to detect islanding. This requires additional communication equipment between DG and the grid, which is a costly option [3]. The local methods can be further divided into passive methods and active methods. The main passive methods include OUF, OUV, voltage vector shift, measurement of total harmonic distortion and rate of change of frequency [1]. When the load and DG powers are balance or even close together, passive methods may not be able to detect islanding and NDZ is large [4], which is the major drawback of passive methods. In active methods the islanding is detected by injecting disturbances into the supply and measurement of system response [1], [5]. The major benefit of using the active methods compared to passive methods is their negligible NDZ, however they scarify the power quality. The most applicable active islanding detection methods with voltage and frequency deviations are active frequency drift (AFD) [6], Sandia frequency shift [7], slip-mode frequency shift [8] and Sandia Voltage shift (SVS) [9]. Reactive power variation (RPV) is another active method, which has recently received significant consideration due to its high performance and simple implementation to drift frequency after islanding occurs [10]-[17]. In spite of its advantages, it has some disadvantages that might occure in a various aspects such as difficulty to set its parameters for different conditions, lack of synchronization for multi DG operation, suffering from NDZ, sacrifice the power quality, and/or complexity in implementation. Also, regardless the advantages for RPV method, it has less sensitivity than voltage amplitude variation, and its islanding detection time are longer than a method with voltage amplitude variation. For this reason, SVS has a fast islanding detection time in comparison with many RPV islanding detection methods. In spite of voltage amplitude variation in SVS method with an effective islanding detection method performance, it might affect the power quality [18]. In [19], an islanding detection method was presented based on AFD, which was combined with the voltage amplitude variation. As discussed in [19], the AFD islanding detection method is unable to perform an islanding detection without a composite with voltage amplitude variation method. It means none of them is able to have an effective islanding detection on their own. Therefore, it can be seen that there is a lack of a proper islanding detection method, which voltage amplitude variation is based on its performance. On the other hand, signal processing methods have recently been employed for islanding detection. For their negligible impact on power quality, they can be competitive with active methods [3]. However, a selection of precise threshold value is difficult for these types of islanding detection methods, which has a negative influence on an effective islanding detection [20]. For these reasons, and with regard to the increasing penetration of microgrid [25], [26], a proper operation of islanding detection method should be updated for a fast performance.

In this paper, a new method is presented to deviate the amplitude of PCC voltage when islanding happens with a negligible effect on power quality. Also, the loading quality factor has minor effect on the performance of the proposed method. Its implementation is simple and independent from the load parameters. It relies on the DG rated active power and grid voltage, which are directly available. The paper is arranged as follows. Section II explains the main criteria/parameters in island mode. Section III proposes the new method for islanding detection. Section IV gives the results of performance and with simulation for the introduced method.

II. Main Criteria/Parameters in Islanding Mode

The system under islanding mode is illustrated in Fig. 1. It shows a three-phase gird and a parallel three-phase RLC load with an inverter-based DG that is modelled as a three-phase inverter after a DC source. The DG interface controllers are including two controllers, an inner current controller and an outer power controller as depicted in Fig. 2. The instantaneous active and reactive powers can be shown in terms of the dq axis components, as (1) and (2) [21].

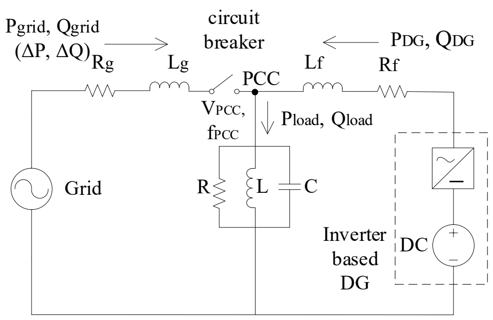

Fig. 1. System study for islanding mode.

$$P_{DG} = \frac{3}{2} v_d i_d \tag{1}$$

$$Q_{DG} = \frac{3}{2} v_d i_q \tag{2}$$

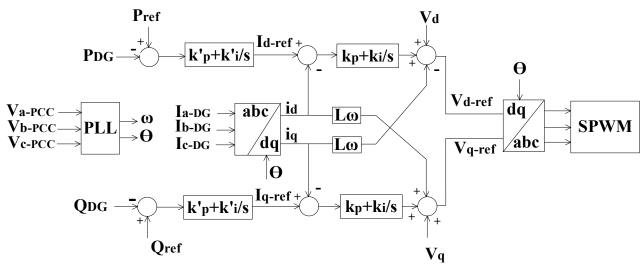

Fig. 2. DG interface controller.

During the grid connection, the active and reactive power of the load are presented as in (3) and (4).

$$P_{load} = \frac{V_{PCC}^2}{R} \tag{3}$$

$$Q_{load} = V_{PCC}^2 \left(\frac{1}{2\pi f_{PCC} L} - 2\pi f_{PCC} C \right) \tag{4}$$

Also, the relationship between active/reactive load powers, DG and the grid can be expressed as in (5) and (6):

$$P_{load} = \Delta P + P_{DG} \tag{5}$$

$$Q_{load} = \Delta Q + Q_{DG} \tag{6}$$

Where, ΔP and ΔQ are the active and reactive power mismatch between DG and load, which are provided by the grid. On the other hand, the relationship between rated voltage, DG active power and max/min of OUV thresholds can be obtained as follows [22]:

$$\left(\frac{V_{rated}}{V_{max}}\right)^2 - 1 \le \frac{\Delta P}{P_{DG-rated}} \le \left(\frac{V_{rated}}{V_{min}}\right)^2 - 1 \tag{7}$$

As shown in (7), if a ratio of power mismatch and rated active power is between the abovementioned intervals, OUV relay is unable for islanding detection and it is located inside NDZ, otherwise OUV relay is able to detect islanding conditions.

III. Proposed Method For Islanding Detection

In accordance with IEEE Std. 929-2000 [23], the OUV relay should be set between 88% and 110% of the grid rated voltage. Therefore, the boundary of (7) can be obtained as (8) [24]:

$$-17.36\% \le \frac{\Delta P}{P_{DG-rated}} \le 29.13\% \tag{8}$$

Thus, for a DG with 100 kW rated active power, equation (8) can be expressed as:

$$-17.36\ kW \le \Delta P \le 29.13\ kW \tag{9}$$

Therefore, the boundary of active load power, when the OUV is within its upper and under thresholds limits will be as (10).

$$82.64\ kW \le P_{load} \le 129.13\ kW \tag{10}$$

The relationship between PCC voltage, load resistance and active load power is illustrated in Fig. 3. It shows that the curve between active load power and PCC voltage is approximated linear in the intervals 88% and 110% of the rated voltage of the grid.

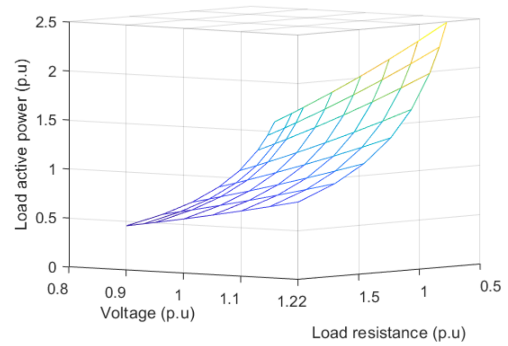

Fig. 3. Relationship between, PCC voltage, load resistance and active load power.

Therefore, the curve of the P-V load can be approximated with a line within the OUV thresholds. In this case, the magnitude of PCC voltage is considered equal to the rated grid voltage, when the active power of the load is balance with rated active power of DG as follows:

$$\frac{P_{load}-1}{V_{PCC}-1}=\frac{dP}{dV} \tag{11}$$

By differentiating (3) and substituting in the right hand of (11), it is obtained:

$$\frac{P_{load}-1}{V_{PCC}-1}=\frac{2V_{PCC}}{R} \tag{12}$$

$$P_{load}=\frac{2V_{PCC}^{2}-2V_{PCC}}{R}+1 \tag{13}$$

$$P_{load}=\frac{2V_{PCC}^{2}-2V_{PCC}}{\frac{V_{PCC}^{2}}{P_{load}}}+1 \tag{14}$$

$$P_{load}=\frac{V_{PCC}}{-V_{PCC}+2} \tag{15}$$

Equation (15) shows the relationship between active power of the load and voltage at PCC. The characteristic of proposed method as the new reference for active power of the DG can be introduced as (16):

$$P_{ref-new}=\frac{aV_{PCC}}{-bV_{PCC}+c} \tag{16}$$

where a, b, and c represent the characteristic of the new active power reference for DG. It is worth noting a, b, and c should be set in such that, the DG is able to detect islanding without a degradation of power quality during the grid connection. In this paper a, b, and c are set at 1.2, 1.4, and 2.6 respectively, as (17). Fig. 4 shows the characteristic of proposed method.

$$P_{ref-new}=\frac{1.2V_{PCC}}{-1.4V_{PCC}+2.6} \tag{17}$$

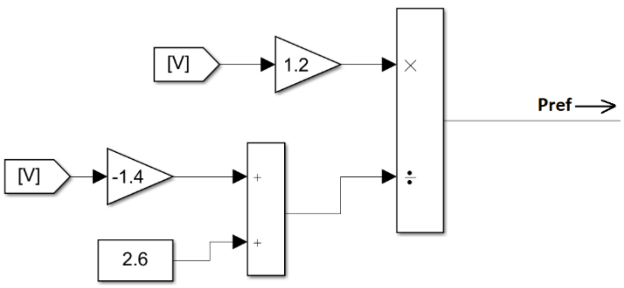

Fig. 4. Proposed method characteristic implementation.

IV. Performance of Simulation Results

In this section, many cases are simulated by using MATLAB/SIMULINK software to test the proposed method for islanding detection with the circuit as depicted in Fig. 1. The grid parameters and inverter controller parameters of DG are shown in Table I. An island occurs at t = 0.3 s. Equation (17) is employed as the active power reference of the DG for islanding detection.

Table I-Grid and DG Parameters.

Grid Parameters	
Voltage, Frequency	400 V, 50 Hz
Grid: Resistance, Inductance	0.02 Ω, 0.3 mH
Inverter Controller Parameters of DG	
Current Controller	kp=3, ki = 60
Power Controller	k'p = 1, k'i = 400
Rated Active Power	100 kW

A. Proposed islanding detection method for different active power mismatch

Based on the IEEE Std. 929-2000 [23], the load is set to a different active loading such as 25%, 50%, 100%, and 125% of rated output of the inverter. The reference reactive power of DG is set at zero (unity power factor) and the loading quality factor is set at 2.5. The simulated cases parameters are shown in Table II.

Table II Parameters of the Load for different active power.

P_{load} (kW)	R (Ω)	L (mH)	C (μF)
25	6.4	2.03	4973.6
50	3.2		
100	1.6		
125	1.28		

Fig. 5 shows the PCC voltage magnitude for the active power of the load, which is set from 25% to 125% rated active power of the DG. The proposed method is able to detect islanding for different active power mismatch with very short detection time. As illustrated in Table III, despite of different values of active power mismatch, all detection times are close together. Fig. 5 shows, when the active load power is less than the active power of DG, PCC voltage rises. Thus, after islanding, PCC voltage moves to the upper of OUV threshold. Also, when the active load power is more than the DG active power, the PCC voltage drops, therefore it deviates to the lower limits of OUV threshold after islanding. Table III shows islanding detection times of the various active powers for the load and DG.

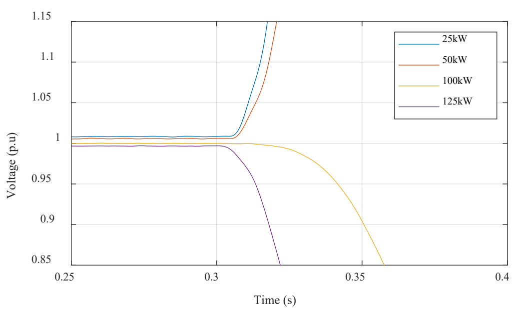

Fig. 5. PCC voltage performance with the proposed method for different active power mismatches.

Table III Detection Time for Different active power mismatch.

Active load power (kW)	Detection time (ms)
25	11
50	13
100	53.5
125	19.5

B. Presented islanding detection method in various reactive power mismatch

With the purpose of confirmation, the capability of presented method for islanding detection with various reactive power mismatch, the impact of PCC frequency change is modelled and discussed in section B. The simulated cases parameters are shown in Table IV. The reference reactive power of DG is set to zero (unity power factor) and the loading quality factor is set at 2.5. Also, the active load power and active power of DG are balance ($\Delta P = 0$).

Table IV Load Parameters for various frequency at PCC.

f_{PCC} (Hz)	R (Ω)	L (mH)	C (μF)
49.8	1.6	2.04	4993.6
50		2.03	4973.6
50.2		2.02	4953.8

Fig. 6 shows the PCC voltage performance, when the frequencies are set before islanding at 49.8 Hz, 50 Hz and 50.2 Hz. It shows that the proposed method ability for islanding detection in a very short time. As the proposed method's characteristic is based on magnitude of PCC voltage, regardless of the PCC frequency value, all three cases are moved to the lower value of OUV threshold until islanding is detected. Table V shows islanding detection time for different PCC frequency.

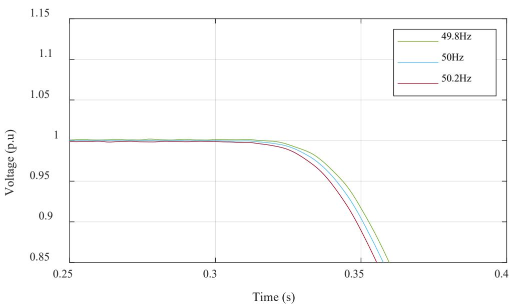

Fig. 6. PCC voltage performance with the proposed method for different PCC frequencies.

Table V Detection Time for Different PCC frequency.

f_{PCC} (Hz)	Detection time (ms)
49.8	55.5
50	53.5
50.2	48.5

C. Proposed islanding detection method for unbalanced load

In this part, the effect of unbalanced loading on the proposed islanding detection method is considered. In the first case, the phase a for the active power of the load is set at 115kW and the phases b and c for the active power of the load are set at 100kW. In the second case, phases a and b are set at 115 kW and phase c is set at 100 kW. For both cases, the load reactance is set for operation at 50 Hz and loading quality factor is set at 2.5. The reactive power reference of DG is set at zero, therefore $\Delta Q = 0$. The simulated parameters are illustrated in Table VI.

Table VI Load Parameters for Different unbalanced loads.

Case	R_a (Ω)	R_b (Ω)	R_c (Ω)	L (mH)	C (μF)
1	1.391	1.6	1.6	2.0372	4973.6
2	1.391	1.391	1.6		

Fig. 7 shows the islanding detection for the unbalanced load. Case 1 shows the unbalance load between phase a and phases b and c, also case 2 shows the unbalanced load for phases a and b with phase c. As shown in Fig. 7, the proposed islanding detection method can detect islanding for unbalanced load with a short detection time. Both cases have almost the same detection time and PCC amplitude voltage is deviated to the lower limit of OUV threshold. Also, it shows that in spite of unbalanced load the amplitude voltage has negligible oscillation during the grid connection. It should be noted both cases are tested under zero reactive power mismatch at 50 Hz, which is a difficult case for islanding detection.

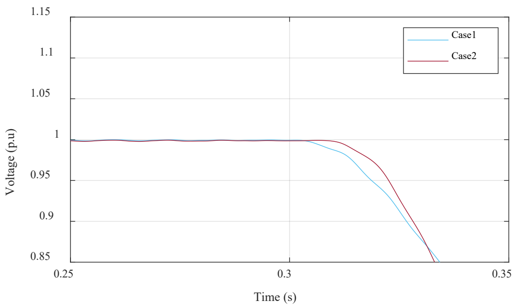

Fig. 7. PCC voltage performance with the proposed method for unbalanced load.

Table VII shows islanding detection time for unbalanced load conditions.

Table VII Detection Time for unbalanced Load.

Case	Detection time (ms)
1	30
2	30.5

D. Proposed islanding detection method for non-unity power factor ($Q_{ref} \neq 0$)

Many cases for DG with zero reactive power have been tested. In this section, DG generates both active power and reactive power together, and the amount of DG reactive power is considered 20% of the DG rated active power (20kVAr). For the first case, the proposed method is tested for balance active power between the load and DG ($\Delta P = 0$). The PCC frequency is set without the reactive power mismatch between the load and DG ($\Delta Q = 0$) as well, with loading quality factor equal 2.5, as the most difficult case. For the second case, the proposed method is modelled with aforementioned values and unbalanced load. The simulated cases parameters are illustrated in Table VIII.

Table VIII Load Parameters for the DG with non-unity power factor.

Case	R_a (Ω)	R_b (Ω)	R_c (Ω)	f_{PCC} (Hz)	L (mH)	C (μF)

1	1.6	1.6	1.6	52.04	2.03	4973.6
2	1.39	1.39	1.6			

As illustrated in Fig. 8, the presented islanding detection method can detect islanding in a short time for both balance and unbalanced load, when the DG providing both active and reactive power together. Compared to section B, it shows that the DG operation with unity and non-unity power factor has similar detection time for the most difficult case, when active/reactive power mismatch is zero. Also, a comparison with part C shows that the DG operation with unity and non-unity power factor has almost the same detection time for unbalanced load. Table IX shows islanding detection times when the DG is generating both active and reactive power together.

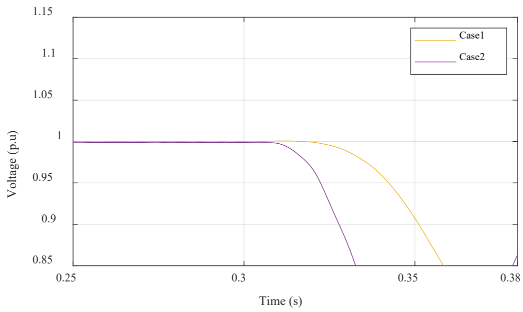

Fig. 8. PCC voltage performance for balance and unbalanced load and the DG with active/reactive power.

Table IX Detection Time for the DG with active/reactive power generating.

Case	Detection time (ms)
1	54
2	30

E. Proposed islanding detection method for different loading quality factors

As stated in the IEEE Std. 929 [23], the loading quality factor can be equal or less than 2.5 ($Q_f \leq 2.5$). Therefore, the proposed islanding detection method is tested for different loading quality factors. The condition of DG is set for the most difficult case, when active/reactive power mismatch is zero. The simulated cases parameters for different loading quality factors are illustrated in Table X.

Table X Load Parameters for different loading quality factors.

f_{PCC} (Hz)	Q_f	R (Ω)	L (mH)	C (µF)
50	0.5	1.6	10.18	994.7
	1		5.09	1989.4
	1.5		3.39	2984.2
	2		2.54	3978.9
	2.5		2.03	4973.6

Fig. 9 shows the PCC voltage performance for different loading quality factors after islanding occurs. Fig. 9 proves that the proposed method has the capability for islanding detection under different loading quality factors. Fig. 9 shows a change in the values of loading quality factor has minimum effect on the islanding detection time. Also, it presents that increasing loading quality factor does not have any effect on the PCC voltage performance. In other words, regardless the value of loading quality factor, there is no impact on the power quality, during the load and the DG connection to the grid. Table XI shows detection time for the various loading quality factors.

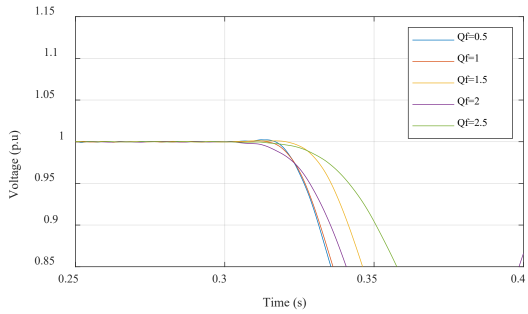

Fig. 9. PCC voltage performance for different loading quality factors.

Table XI Detection Time for a Various Loading Quality Factors.

Q_f	Detection time (ms)
0.5	33
1	33.1
1.5	43.5
2	37.5
2.5	53.5

V. Conclusion

A new islanding detection method with voltage amplitude variation has been presented in this paper. The characteristic of presented method is independent from the load variables and PCC frequency. Therefore, its implementation is simple, and its parameters can properly be set for any DG with different rated active powers. Many cases have been examined to confirm the proposed method performance. An OUV relay is adequate to detect islanding for a DG equipping with the proposed method, which reduces the complexity and the cost of its implementation. The proposed method has zero NDZ for a wide range of loading quality factors. In addition, it has the capability of maintaining stable operation under unbalanced load conditions. The proposed method has superior performance when there is zero mismatch between the DG and load. The detection times are very short for all cases, and a change in the load conditions such as increasing loading quality factor has minor effect on the detection time.

References

[1] K. Naraghipour, K. Ahmed and C. Booth, "A Comprehensive Review of Islanding Detection Methods for Distribution *Systems," in Proc. 9th Int. Conf. on Renewable Energy Research and Application (ICRERA), 2020, pp. 428-433.*

[2] Institute of Electrical and Electronics Engineers, "IEEE 1547- Standard for Interconnection and Interoperability of Distributed Energy Resources with Associated Electric Power Systems Interfaces," New York, February 2018.

[3] S. K.G. Manikonda, and D.N. Gaonkar, "Comprehensive review of IDMs in DG systems," *IET Smart Grid*, pp. 11-24, Apr. 2019.

[4] M.S. Kim, R. Haider, G.J. Cho, C.H. Kim, C.Y. Won, Y., and J.S. Chai, "Comprehensive review of islanding detection methods for distributed generation systems," *Energies*, p. 837, Jan. 2019.

[5] A. M. Massoud, K. H. Ahmed, S. J. Finney, and B. W. Williams, "Harmonic distortion-based island detection technique for inverter-based distributed generation," IET Renewable Power Generation, vol. 3, no. 4, pp. 493-507, Dec. 2009.

[6] A. Yafaoui, B. Wu and S. Kouro, "Improved active frequency drift anti-islanding detection method for grid connected photovoltaic systems," *IEEE transactions on power electronics,* vol. 27, no. 5, pp. 2367-2375, May 2012.

[7] H. Vahedi and M. Karrari, "Adaptive fuzzy sandia frequency-shift method for islanding protection of inverter-based distributed generation," *IEEE transactions on power delivery,* vol. 28, no. 1, pp. 84-92, Oct. 2012.

[8] D. U. Kim and S. Kim "Anti-Islanding Detection Method Using Phase-Shifted Feed-Forward Voltage in Grid-Connected Inverter," *IEEE Access,* vol. 7, pp. 147179-147190, Oct. 2019.

[9] M. El-Moubarak, M. Hassan and A. Faza, "Performance of three islanding detection methods for grid-tied multi-inverters," *IEEE 15th International Conference on Environment and Electrical Engineering (EEEIC)*, pp. 1999-2004, 2015.

[10] H. H. Zeineldin, "A Q–f Droop Curve for Facilitating Islanding Detection of Inverter-Based Distributed Generation," *IEEE transactions on power electronics,* vol. 24, no. 3, pp. 665-673, March 2009.

[11] J. Zhang, D. Xu, et al., "An improved islanding detection method for a grid-connected inverter with intermittent bilateral reactive power variation," *IEEE transactions on power electronics,* vol. 28, no. 1, pp. 268-278, April 2012.

[12] Y. Zhu, D. Xu, et al., "A novel RPV (reactive-power-variation) antiislanding method based on adapted reactive power perturbation," *IEEE transactions on power electronics,* vol. 28, no. 11, pp. 4998-5012, Feb. 2013.

[13] X. Chen and Y. Li, "An Islanding Detection Method for Inverter-Based Distributed Generators Based on the Reactive Power Disturbance,", *IEEE Transactions on Power Electronics*, vol. 31, no. 5, pp. 3559-3574, May 2016.

[14] F. J. Lin, Y. S. Huang, et al., "Active islanding detection method using d-axis disturbance signal injection with intelligent control," *IET Generation, Transmission & Distribution, vol. 7, no. 5,* pp. 537-550, May 2013.

[15] P. Gupta, R. S. Bhatia and D. K. Jain, "Average absolute frequency deviation value based active islanding detection technique," *IEEE Transactions on Smart Grid,* vol. 6, no. 1, pp. 26-35, Aug. 2014.

[16] X. Chen and Y. Li, "An islanding detection algorithm for inverter-based distributed generation based on reactive power control," *IEEE transactions on power electronics,* vol. 29, no. 9, pp. 4672-4683, Oct. 2014.

[17] X. Chen, Y. Li, and P. Crossley, "A novel hybrid islanding detection method for grid-connected microgrids with multiple inverter-based distributed generators based on adaptive reactive power disturbance and passive criteria," *IEEE Transactions on Power Electronics*, vol. 34, no. 9, pp.9342-9356, Dec. 2018.

[18] PVPS, IEA, "Evaluation of islanding detection methods for photovoltaic utility-interactive power systems," Report IEA PVPS T5-09, 2002.

[19] Y. Li, M. Hou, H. Feng and X. Liu, "Composite islanding detection method based on the active frequency drift and voltage amplitude variation," *IEEE PES Asia-Pacific Power and Energy Engineering Conference (APPEEC)*, pp. 1-6, 2014.

[20] S. Raza, H. Mokhlis, H. Arof, J. A. Laghari, and L. Wang, " Application of signal processing techniques for islanding detection of distributed generation in distribution network: A review," *Energy Conversion and Management* 96, pp. 613-624, May 2015.

[21] A. Yazdani and R. Iravani, "Voltage-sourced converters in power systems: monitoring, control, and applications," John Wiley & Sons, March 2010.

[22] R. Teodorescu, M. Liserre and P. Rodriguez, "Grid converters for photovoltaic and wind power systems," John Wiley & Sons, July 2011.

[23] IEEE Recommended Practice for Utility Interface of Photovoltaic (PV) Systems, IEEE Standard 929-2000, Apr. 2000.

[24] Z. Ye, Miller, A. Kolwalkar, Y. Zhang, P. Du and R. Walling, "Evaluation of anti-islanding schemes based on nondetection zone concept," IEEE transaction on power electronics, vol. 19, no. 5, pp. 1171-1176, Sep. 2004.

[25] A. Bani-Ahmed and A. Nasiri, "Development of real-time hardware-in-the-loop platform for complex microgrids," *International Conference on Renewable Energy Research and Applications (ICRERA)*, pp. 994-998, Palermo – Italy, 2015.

[26] C. Natesan, et al., "Power Management Strategies in Microgrid: A Survey". *International Journal of Renewable Energy Research (IJRER)*, vol. 5, no. 2, pp. 334-40, Jun 2015.